Permeability and single channel conductance of human homomeric ρ1 $GABA_C$ receptors

Virginia E. Wotring, Yongchang Chang and David S. Weiss

Department of Neurobiology, University of Alabama at Birmingham, 1719 Sixth Avenue South, CIRC 410, Birmingham, AL 35294, USA

(Received 19 April 1999; accepted after revision 24 September 1999)

1. Homomeric human ρ1 $GABA_C$ receptors were expressed in *Xenopus* oocytes and in human embryonic kidney cells (HEK293) in order to examine their conductance and permeability.

2. Reversal potentials of currents elicited by γ-aminobutyric acid (GABA) were measured in extracellular solutions of various ionic composition to determine relative permeability of homomeric ρ1 receptors. The rank order of anionic permeability was: $SCN^- > I^- > NO_3^- > Br^- > Cl^-$ > formate (For^-) > HCO_3^- > acetate (Ac^-) ≈ proprionate ($Prop^-$) ≈ isethionate (Ise^-) ≈ F^- ≈ PO_4^-.

3. In the oocyte expression system, relative permeabilities to SCN^-, I^-, NO_3^-, Br^- and HCO_3^- were higher for ρ1 $GABA_C$ receptors than $\alpha1\beta2\gamma2L$ $GABA_A$ receptors.

4. Expression of ρ1 $GABA_C$ receptors in *Xenopus* oocytes and in HEK293 cells gave similar relative permeabilities for selected anions, suggesting that the expression system does not significantly alter permeation properties.

5. The pore diameter of the homomeric ρ1 $GABA_C$ receptor expressed in oocytes was estimated to be 0·61 nm, which is somewhat larger than the 0·56 nm pore diameter estimated for $\alpha1\beta2\gamma2L$ $GABA_A$ receptors.

6. Homomeric ρ1 GABA receptors expressed in oocytes had a single channel chord conductance of 0·65 ± 0·04 pS (mean ± S.E.M.) when the internal chloride concentration ($[Cl^-]_i$) was 20 mM. With a $[Cl^-]_i$ of 100 mM, the single channel chord conductance was 1·59 ± 0·24 pS.

7. The mean open time directly measured from 43 GABA-induced channel openings in six patches was 3·2 ± 0·8 s. The mean open time in the presence of 100 μM picrotoxin was 0·07 ± 0·01 s (77 openings from 3 patches).

8. The differences observed in ionic permeabilities, pore size, single channel conductance and mean open time suggest that the ρ1 homomeric receptor may not be the native retinal $GABA_C$ receptor reported previously.

$GABA_C$ receptors are chloride-selective γ-aminobutyric acid (GABA)-gated channels that are abundant in the retina (Enz *et al.* 1995, 1996; Yeh *et al.* 1996) and have also been found in the brain (Enz *et al.* 1995; Albrecht *et al.* 1997; Wegelius *et al.* 1998). While $GABA_C$ receptors have been studied primarily in the retina, there are reports of $GABA_C$-like responses in frog optic tectum, rat cerebellar granule cells, and rat hippocampal neurons during early development (Sivilotti & Nistri, 1989; Strata & Cherubini, 1994; Martina *et al.* 1997). Three ρ subunits have been cloned (ρ1, ρ2 and ρ3) that show significant homology with $GABA_A$ receptor subunits and other subunits from this superfamily of ligand-gated ion channels (Cutting *et al.* 1991; Wang, 1994; Ogurusu & Shingai, 1996). $GABA_C$ receptors are thought to be composed of some combination of ρ subunits, but the subunit identity and the stoichiometry are not yet known. It is possible that native $GABA_C$ receptors could be composed of ρ homomeric receptors, or that the ρ subunits could assemble into heteromers with each other, and/or other subunits. It has been shown that functional homomeric $GABA_C$ receptors can form in expression systems (Polezani *et al.* 1991; Kusama *et al.* 1993). The homomeric ρ1 receptor is a strong candidate for a native $GABA_C$ receptor because in exogenous expression systems the receptors have properties similar to those of native $GABA_C$ receptors.

At present, our understanding of $GABA_C$ receptor function is limited, but it has been established that they are different from other GABA-gated channels in several ways. $GABA_C$ receptors are activated by much lower concentrations of agonist than $GABA_A$ receptors. In

addition, their deactivation rate is much slower (Amin & Weiss, 1994). In contrast to $GABA_A$ receptors, there is very little desensitization of current with continued agonist application. $GABA_C$ currents are not inhibited by bicuculline, the classical $GABA_A$ antagonist, nor are they modulated by benzodiazepines or barbiturates (Shimada *et al.* 1992). Furthermore, the single channel conductance of retinal native $GABA_C$ receptors is considerably smaller than that of $GABA_A$ receptors (Feigenspan *et al.* 1993).

The purpose of this study was to conduct a comprehensive examination of the permeation and conduction properties of the homomeric $\rho1$ receptor. A comparison was made in order to determine whether the characteristics of $\rho1$ homomers were consistent with what has been reported for native retinal $GABA_C$ receptors. If there are significant permeability and conductance differences between $\rho1$ receptors and $\alpha\beta\gamma$ $GABA_A$ receptors, then future studies via mutagenesis may be directed at elucidating the structural elements responsible for these functional properties.

METHODS

cDNA cloning and *in vitro* transcription

The cDNA encoding the wild-type $\rho1$, $\alpha1$, $\beta2$, or $\gamma2L$ subunits were cloned into pALTER (Promega, Madison, WI, USA). The cDNA was linearized, and cRNA was synthesized using standard *in vitro* transcription techniques as described previously (Amin & Weiss, 1994). Yield and integrity of cRNA were verified by agarose gel electrophoresis.

Oocyte preparation and microinjection

Female *Xenopus laevis* (Xenopus I, Ann Arbor, MI, USA) were anaesthetized by immersion in 0·2% MS-222, and several lobes of ovary were surgically removed. The incision was sutured, and the animal was monitored during the recovery period, after which it was returned to its tank. This procedure was approved by the UAB Animal Welfare Committee. Oocytes were removed not more than 3 times from any animal, with several weeks healing allowed between each procedure. Following the last collection frogs were anaesthetized as above and killed by decapitation. Ovarian lobes were placed in a calcium-free oocyte Ringer solution (OR2) that consisted of (mM): NaCl, 92·5; KCl, 2·5; $MgCl_2$, 1; Na_2HPO_4, 1; 4-(2-hydroxyethyl)-1 piperazine ethanesulfonic acid (Hepes), 5; supplemented with 50 units ml^{-1} penicillin and 50 $\mu g\ ml^{-1}$ streptomycin; pH 7·5. The ovarian lobes were cut into small pieces, and then digested in 0·3% collagenase A (Boehringer Mannheim, Indianapolis, IN, USA) in the above solution. After dispersal (typically about 2 h), stage VI oocytes were selected and thoroughly rinsed and maintained in OR2 with Ca^{2+} (1 mM) at 18 °C for several hours before cRNA injection. Typically, 60–100 nl of cRNA (25–100 ng μl^{-1}) was injected into *Xenopus* oocytes with a Nanoject (Drummond Scientific Co., Broomall, PA, USA); the oocytes were then incubated at 18 °C. Since high expression levels were desired for single channel recording, a larger volume of cRNA solution (about 100 nl) was injected. In this case, the oocytes were incubated in a 150% concentrated incubation solution for 5 min before injection to allow them to shrink slightly to accommodate the injection volume. One day after injection, the oocytes were screened under voltage clamp conditions for expression of GABA receptors. Only oocytes with high expression levels (GABA-induced current larger than 2000 nA) were selected for single channel recording. Lower expression levels (GABA-induced currents between 200 and 1000 nA) were used for reversal potential experiments in order to minimize the error due to series resistance (< 4% at 1000 nA).

HEK293 expression

Human embryonic kidney cells (HEK293) (CRL-1573, American Type Culture Collection, Rockville, MD, USA) were grown in DMEM/F12 supplemented with 10% fetal bovine serum (Atlanta Biologicals, Norcross, GA, USA), 100 units ml^{-1} penicillin and 100 mg ml^{-1} streptomycin in a 37 °C incubator with 95% air and 5% CO_2. At 50–90% confluence, the cells were dispersed with 0·05% trypsin and plated onto poly-L-lysine-coated coverslips in 35 mm culture dishes. The $\rho1$ subunit was subcloned into the mammalian expression vector pcDNA3 (Invitrogen, San Diego, CA, USA) for transfection. Each dish was transfected for 2 h with $\rho1$ cDNA + pGreenLantern (Promega) using Lipofectamine (Life Technologies, Gaithersburg, MD, USA). A total of 2 μg DNA was used in each 35 mm culture dish. Dishes were then incubated for 48 h before electrophysiological recordings were made. Cells that fluoresced were used for all experiments. All cell culture chemicals were purchased from Life Technologies, unless otherwise stated.

Voltage clamp experiments

The oocyte was placed in a small volume chamber with a continuous perfusion system, as described previously (Amin & Weiss, 1994). The normal extracellular OR2 consisted of (mM): NaCl, 92·5; KCl, 2·5; $MgCl_2$, 1; $CaCl_2$, 1; Hepes, 5; pH 7·5. This could be switched to provide various experimental conditions. Recording microelectrodes were fabricated from thin-walled glass micropipettes (A-M Systems, Carlsborg, WA, USA) on a Sutter Instruments P87 horizontal puller (Novato, CA, USA) and filled with 3 M KCl with a resistance of 1–3 MΩ. In order to prevent fluctuating junctional potentials during ion substitution experiments, the ground electrode was placed in a separate 3 M KCl well connected to the bath by an agar bridge. Solutions for ion replacement experiments had 50 mM of the usual NaCl replaced with 50 mM of one of the following: sodium thiocyanide, sodium iodide, sodium bromide, sodium formate, sodium bicarbonate, monobasic sodium phosphate, sodium proprionate, sodium fluoride, sodium isethionate, caesium chloride (Gibco BRL, Gaithersburg, MD, USA) or lithium chloride. GABA (Calbiochem, LaJolla, CA, USA) was added to these solutions to a final concentration of 1 or 0·5 μM. Each oocyte was allowed to equilibrate at a holding potential of −70 mV in each solution for approximately 1 min before recording sequences were begun. A group of five voltage ramps was applied from −70 mV to +10 mV (except when indicated) and then averaged. Each individual ramp lasted 1 s with 3 s intervals between ramps. The solution was then switched to a GABA-containing solution with the same ionic composition. When the GABA response reached steady state, another group of ramps was taken and averaged. This was followed by a third set of ramps after complete recovery from the GABA application (Fig. 1, inset). For determination of the reversal potential, the initial and recovery ramps were averaged, and this average control ramp was subtracted from the average ramp during GABA application. The voltage at which this GABA minus control ramp crossed the x-axis was the reversal potential of the GABA-induced portion of the current (Fig. 1).

The internal chloride concentration of our oocytes was calculated from our measured chloride (GABA-induced) reversal potentials using constant potassium and calcium concentrations, and a

relative chloride permeability of 1 in the following rearrangement of the Goldman–Hodgkin–Katz (GHK) equation:

$$[Cl^-]_i = [Cl^-]_o \exp(V_{rev}F/RT), \quad (1)$$

where V_{rev} is the mean chloride reversal potential, F is Faraday's constant, R is the gas constant and T is absolute temperature. With our solutions, and a V_{rev} of −20·6 mV, the calculated internal chloride concentration ($[Cl^-]_i$) was estimated to be 43·5 mM.

The permeability (P) of other ions relative to chloride was calculated as follows from the Goldman–Hodgkin–Katz equation (Goldman, 1943; Hodgkin & Katz, 1949) using our calculated internal chloride concentration and the known concentrations for external chloride and replacement ions:

$$\frac{P_{anion}}{P_{Cl}} = \frac{[Cl^-]_i \exp(V_{rev}F/RT) - [Cl^-]_o}{[anion]_o}. \quad (2)$$

The intracellular concentration of the test ion was assumed to be negligible. Reversal potentials were measured in OR2 at the beginning (−20·8 ± 0·8 mV, $n = 6$, where n is the number of times an experimented was repeated) and end (−20·9 ± 0·4 mV, $n = 6$) of the experiment and were virtually identical indicating that the internal concentration of chloride remained relatively stable, even though the extracellular chloride concentration was changed many times during the course of the experiment. We used eqn (2) with 50 mM of the substituted anion in the external fluid ($[anion]_o$) and an internal chloride concentration of 43·5 mM to calculate the anionic permeability (P_{anion}) relative to chloride for each anion substitution. Student's t test was used for comparisons between chloride permeability and the permeability to other anions. With this equation, the relative test ion permeability is zero at a reversal potential of −4·2 mV. In order to estimate the diameter of the pore (D_p), the relative permeabilities (P_{anion}/P_{Cl}), along with the Stokes diameters (d) of the ions, were used to fit the following equation with a non-linear least-squares algorithm in Igor (WaveMetrics, Lake Oswego, OR, USA):

$$\frac{P_{anion}}{P_{Cl}} = x\left(1 - \frac{d}{D_p}\right)^2, \quad (3)$$

where x is an arbitrary vertical scaling factor for fitting. Relative permeabilities for Br^-, Cl^-, For^-, HCO_3^- and Ac^- were used for the fit, as Stokes diameters of these large ions can be estimated most accurately due to their small hydration shells (Bormann *et al.* 1987).

Whole-cell voltage clamp recordings were obtained from HEK293 cells with an Axopatch 1D amplifier (Axon Instruments, Foster City, CA, USA). The recording chamber was perfused with a solution containing (mM): NaCl, 150; Hepes, 4; KCl, 4; $CaCl_2$, 2; $MgCl_2$, 2; pH 7·4. The extracellular solution was changed to one with 75 mM NaCl replaced by 75 mM NaSCN or NaI. GABA (final concentration, 1 mM) was mixed in each of these solutions and applied via a piezo-driven θ tube positioned near the cell. Electrodes were pulled in two steps on a List vertical puller (Great Neck, NY, USA) from thick-walled borosilicate glass (Sutter Instruments). Electrodes were filled with solution containing (mM): CsCl, 130; tetraethylammonium chloride, 10; Hepes, 10; EGTA, 1·1; glucose, 4; pH 7·2. Data were filtered at 200 Hz and digitized at 2000 Hz. The steady-state response to GABA was measured at a series of holding potentials.

Single channel recording

Two to 5 days after injection, the vitelline membrane of the oocyte was peeled off with fine forceps in normal extracellular solution. The oocyte was then put into a recording chamber made from a 35 mm Petri dish. To eliminate suction noise, continuously flowing extracellular solution was drained by gravity with a piece of tubing connected to a hole in the side wall of the chamber. The outlet of the tubing was connected to a glass tube with an adjustable outlet level. Fine glass filaments were attached to the outside of the glass tube outlet to reduce surface tension effects and allow the solution level in the chamber to be smoothly adjusted to any level. This perfusion system greatly reduced noise; noise reduction proved necessary for successful recordings of the very small conductance ρ1 receptors.

Recording electrodes were pulled with a vertical puller (List) in two steps from borosilicate glass tubes (1·5 mm o.d., 0·8 mm i.d.; A-M Systems). The tip of the electrode was coated with Sylgard (Dow Corning, Midland, MI, USA) and then fire polished to a diameter of ~1 μm with a microforge (Narashige, Japan). To minimize noise, the electrodes were filled to a level of less than 10 mm from the tip with an intracellular solution which contained (mM): KCl, 20; KF, 80; EGTA, 10; Hepes, 10; pH 7·2. Potassium fluoride was used in the pipette solution to facilitate outside-out patch formation (Methfessel *et al.* 1986). The electrodes had resistances of about 10 MΩ. For macropatch experiments, we used electrodes with a larger diameter (~5 μm). Unless otherwise stated, the extracellular solution consisted of (mM): NaCl, 98·5; KCl, 2·5; $MgCl_2$, 2; $CaCl_2$, 1 pH 7·2. For the 100 mM intracellular Cl^- experiments, the intracellular solution contained (mM): KCl, 100; EGTA, 10; Hepes, 10; pH 7·2; the extracellular solution contained (mM): CsCl, 100; $MgCl_2$, 1; $CaCl_2$, 1; Hepes, 10; pH 7·2.

The drug application was controlled with a fast-switching piezo system. A control solution (blank or with GABA) and an experimental solution (GABA or GABA plus picrotoxin) were connected through polyethylene tubing to a glass θ tube. Different concentrations of drug could be selected on each side of the θ tube by switching a six-way valve. Two solutions were perfused into the chamber continuously, one on each side of the θ tube. The control solution was directed to the patch first, then the computer-controlled piezo translator moved the θ tube so that the test solution was directed at the patch. The current was amplified by an Axopatch 200A amplifier (Axon Instruments), low-pass filtered at 200 Hz with an eight-pole Bessel filter (Frequency Devices, Haverhill, MA, USA), and then digitized at 2000 Hz with 16-bit resolution for further analysis by using the ITC-16 computer interface (Instrutech, Greatneck, NY, USA) running Igor software (Wavemetrics) in conjunction with a set of macros to drive the board (Bob Wyttenbach, Cornell University, Ithaca, NY, USA) in a Macintosh computer (Apple Computer, Cupertino, CA, USA). Although fast channel closures are missed at this filter setting (thus increasing our estimates of the mean open time), it was necessary in order to resolve channel openings from baseline noise.

Since the single channel current was very small, we determined the single channel current by fitting a Gaussian distribution function to an all-points histogram of each trace. The difference between the two consecutive means is the single channel current. The single channel chord conductance of GABA-induced openings was then calculated from the single channel currents and the predicted reversal potential according to the following equation:

$$\gamma = \frac{i}{V_m - E_{Cl}}, \quad (4)$$

where single channel chord conductance (γ) is equal to the single channel current divided by the driving force, which is the difference between the membrane voltage (V_m) and the chloride reversal

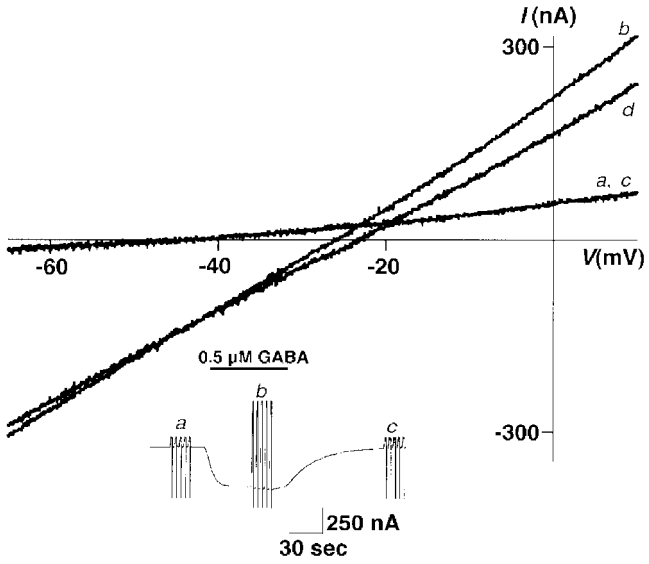

Figure 1. A ramp protocol was used to determine reversal potentials of GABA-induced currents
The holding potential was ramped from −70 mV to +10 mV over a period of 1 s and repeated five times in rapid succession. Each trace shown is the average of these five. *a* and *c*, control ramps before GABA application and after recovery, respectively, are superimposed. *b*, ramp during steady-state application of 0·5 μM GABA. *d*, GABA ramp after subtraction of the average of *a* and *c* (control ramps). Note that the point at which the GABA ramp and the control ramp cross is the reversal potential of the GABA-induced current and is the same as where the subtracted ramp crosses the *x*-axis. Inset, current trace of two-electrode voltage clamp ramp experiment in an oocyte, showing the sets of five ramps before, during, and after recovery from GABA application, which were averaged to obtain the ramps labelled *a*, *b* and *c* in the main figure.

potential (E_{Cl}). The membrane voltage was calculated using the known concentrations of chloride in the internal and extracellular solutions, with fluoride permeability assumed to be zero. The ensemble average was calculated from traces with time-locked GABA applications. The small single channel conductance precluded a detailed kinetic analysis. Therefore, for determination of open time, we directly measured limited numbers of channel openings and averaged them to obtain a mean open time. All results are presented as means ± S.E.M.

RESULTS

Oocyte ramps show linear current–voltage relationship

Two-electrode voltage clamp of oocytes injected with ρ1 cRNA resulted in GABA-induced inward currents that reached equilibrium slowly and showed no signs of desensitization (Fig. 1, inset). Before GABA application, five ramps from −70 mV to +10 mV were averaged to obtain trace *a* in Fig. 1. The solution was then switched to 500 nM GABA. When the GABA current had reached equilibrium, five ramps were performed and averaged to obtain trace *b* (Fig. 1). This was followed by a return to control solution and recovery ramps (Fig. 1, trace *c*). Trace *d* in Fig. 1 is the GABA-induced portion of the ramp current obtained by taking the difference between GABA and control ramps. Currents in oocytes exhibited linear current–voltage relationships in the absence or presence of GABA. In normal OR2 the reversal potential of the GABA-induced portion of the current (Fig. 1, trace *d*) was −20·63 ± 0·40 mV (mean ± S.E.M., $n = 35$). Reversal potentials were unchanged when

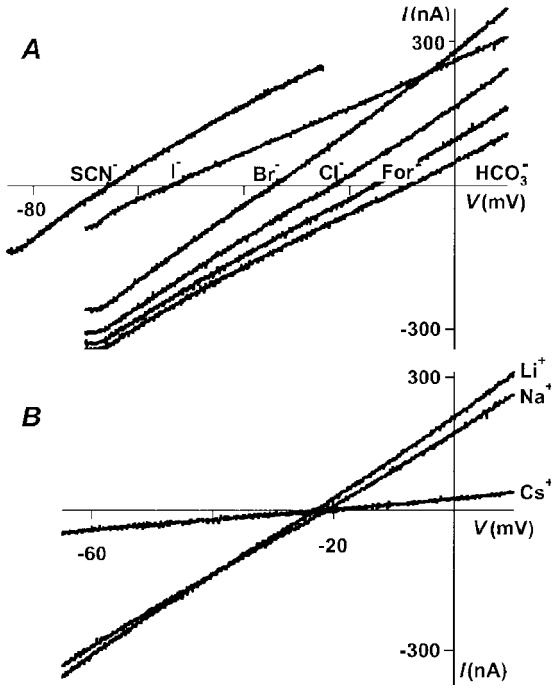

Figure 2. Reversal potentials are shifted by anion substitutions but not by cation substitutions
A, 50 mM NaCl in the extracellular solution was replaced by 50 mM sodium salt of the anion indicated by each trace. The holding potential was ramped from −70 mV to +10 mV over a period of 1 s, except in the case of SCN^-, when a ramp from −85 mV to −25 mV was used. *B*, a similar experiment, varying the cation composition of the extracellular solutions.

various concentrations of GABA were applied (data not shown); the reversal potential was not dependent on current amplitude and may be determined at any point along the dose–response relationship. In addition, reversal potentials were the same when the ramps were run in the reverse direction (from +10 mV to −70 mV), indicating that ρ1 $GABA_C$ receptors show no significant hysteresis (data not shown).

Reversal potentials are shifted by anions, but not by cations

When the extracellular fluid was altered so that ~50% of the chloride was replaced by an equimolar amount of a different anion, the reversal potentials were altered from the −20 mV measured in normal OR2 (Fig. 2*A*). The reversal potentials of GABA currents elicited in bromide (−32·5 ± 1·1 mV, $n = 10$), iodide (−50·5 ± 1·4 mV, $n = 21$), nitrate (−47·6 ± 0·4 mV, $n = 3$) and thiocyanate (−65·5 ± 1·9 mV, $n = 12$) are all more negative than that for chloride, indicating that these ions are all more permeable than chloride. Formate (−14·9 ± 0·7 mV, $n = 13$), bicarbonate (−9·0 ± 0·6 mV, $n = 14$), acetate (−6·3 ± 1·0 mV, $n = 15$), proprionate (−5·8 ± 0·8 mV, $n = 15$), isethionate (−5·2 ± 0·8 mV, $n = 5$), fluoride (−4·7 ± 0·7 mV, $n = 5$), and phosphate (−4·3 ± 1·0 mV, $n = 16$) all shifted the reversal potential to more positive values (Fig. 2*A* and Table 1), indicating that they are less permeable than chloride. We found that the maximum GABA-induced current in the 50 mM iodide solution was about 75% of the maximum current in the other solutions, leading to the shallow slope of the iodide ramp. Current amplitudes in the other anions tested were roughly similar to those seen in normal OR2. Not surprisingly, cation replacement experiments showed that the reversal potential was not significantly changed (Fig. 2*B*; NaCl, −20·6 ± 0·4 mV, $n = 35$; LiCl, −21·7 ± 0·8, $n = 7$; CsCl, −22·3 ± 0·9, $n = 8$; *N*-methyl-D-glucamine (NMDG), −17·5 ± 2·1, $n = 3$), indicating that the ρ1 channel was essentially cation impermeable. The GABA dose–response curve was shifted to the right in 50 mM caesium solutions; the GABA EC_{50} was 2·6 ± 0·7 μM ($n = 4$) as opposed to 0·9 ± 0·1 μM ($n = 9$) in normal OR2. This reduced sensitivity to GABA was responsible for the shallow ramp in caesium solutions.

Table 1. Effects of 50 mM ion replacement on reversal potentials and relative permeabilities

	Reversal potential (mV)	Relative permeability	*n*
SCN^-	−65·49 ± 1·92	11·53 ± 0·89	12
I^-	−50·51 ± 1·35	5·81 ± 0·37	21
NO_3^-	−47·63 ± 0·23	4·74 ± 0·37	3
Br^-	−32·47 ± 1·07	2·31 ± 0·13	11
Cl^-	−20·63 ± 0·40	1	35
For^-	−14·90 ± 0·67	0·58 ± 0·04	13
HCO_3^-	−8·99 ± 0·55	0·27 ± 0·03	14
Ac^-	−6·33 ± 1·00	0·15 ± 0·04	15
$Prop^-$	−5·76 ± 0·75	0·12 ± 0·03	16
Ise^-	−5·18 ± 0·75	0·08 ± 0·03	5
F^-	−4·74 ± 0·66	0·06 ± 0·03	5
PO_4^-	−4·26 ± 0·98	0·06 ± 0·04	15

Reversal potentials and relative permeabilities of ρ1 receptors expressed in oocytes were determined in various ionic conditions. The reversal potentials of GABA-induced currents were measured in solutions with 50 mM (approximately 50%) of the sodium chloride replaced by the sodium salt of the indicated anion. Relative permeabilities were calculated using a rearrangement of the GHK equation as described in the text. Values are means ± S.E.M.; *n* is the number of cells tested.

Rank order of ionic permeability

Relative ion permeabilities can be determined using reversal potentials measured at known ion concentrations and the GHK equation (Goldman, 1943; Hodgkin & Katz, 1949). In homomeric ρ1 receptors, the rank order of permeability was $SCN^- > I^- > NO_3^- > Br^- > Cl^- > For^- > HCO_3^- > Ac^- \approx$ proprionate ($Prop^-$) ≈ isethionate (Ise^-) ≈ $F^- \approx PO_4^-$. In order to compare ρ1 receptors directly with $GABA_A$ receptors, we used this ramp protocol with oocytes injected with α1, β2 and γ2 cRNAs. The same rank order of permeability was seen (Fig. 3), and the permeability values obtained with this method were very similar to those previously published for native spinal cord $GABA_A$ receptors (Bormann *et al.* 1987). Interestingly, the relative

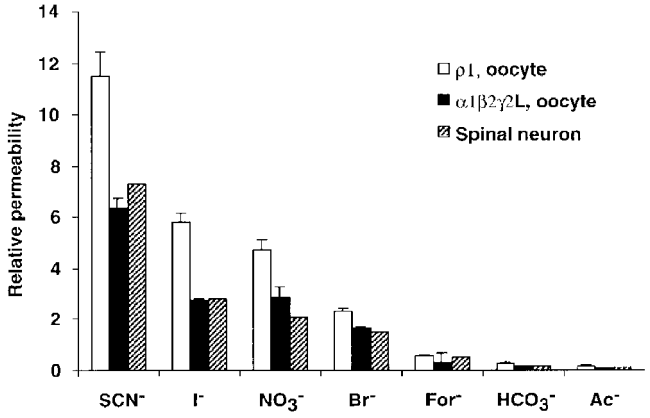

Figure 3. Comparison of the relative permeabilities to anions of ρ1 receptors and $GABA_A$ receptors

For most of the anions tested, relative permeabilities of ρ1 receptors were higher than $GABA_A$ receptors in our oocyte expression system. Permeabilities of α1β2γ2L expressed in oocytes to SCN^-, I^-, NO_3^-, Br^- and HCO_3^- were significantly different from the ρ1 permeabilities. The corresponding permeabilities reported by Bormann (1987) from spinal cord neurons are provided for comparison to our results. α1β2γ2L expressed in oocytes has essentially the same permeability profile as native spinal neurons.

Table 2. Relative permeabilities of ρ1 receptors in different expression systems

	SCN^-	I^-
Xenopus oocytes	11·53 ± 0·89 (n = 12)	5·81 ± 0·37 (n = 21)
HEK293 cells	10·48 ± 1·05 (n = 5)	5·13 ± 0·41 (n = 5)

Reversal potentials were measured in solutions containing 50% NaCl replaced by NaI or NaSCN as described in the text. Relative permeabilities were then calculated using these reversal potentials. There was no significant difference in permeabilities to these anions in the different expression systems tested ($P > 0·2$). Values are means ± S.E.M., with the number of cells given in parentheses.

permeabilities to SCN^-, I^-, NO_3^-, Br^- and HCO_3^- were significantly greater in ρ1 $GABA_C$ receptors than in $\alpha1\beta2\gamma2L$ $GABA_A$ receptors ($P < 0·05$, $n = 4$). In order to establish if the permeabilities we measured were affected by the oocyte expression system, we repeated the SCN^- and I^- experiments in HEK293 cells, and the relative permeabilities were similar to those measured in oocytes (Table 2), suggesting that the expression system does not significantly alter permeation properties.

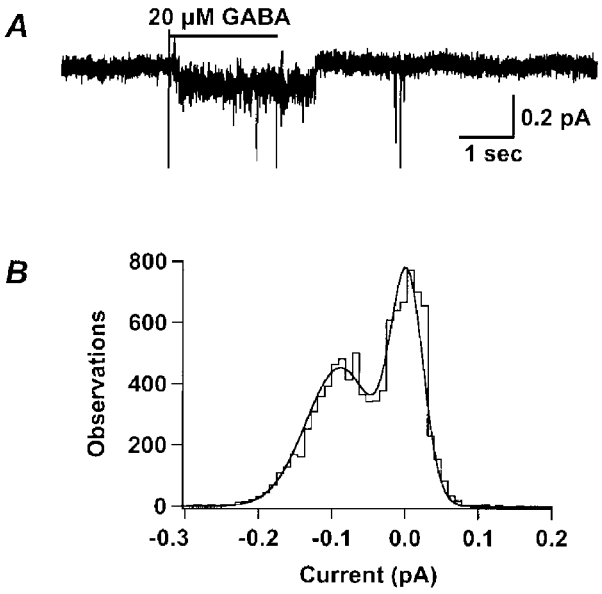

Figure 4. The ρ1 GABA-induced single channel conductance is small

A, GABA (20 μM) induced a single channel current in an excised outside-out patch from an oocyte expressing homomeric ρ1 GABA receptors. The membrane voltage of the patch was clamped to −200 mV in order to maximize the amplitude of channel openings. Even at this extreme holding potential, the single channel current was only ~0·1 pA. Note that the channel remains open after the end of the GABA application. *B*, the all-points amplitude histogram of the current in *A* shows two peaks. The continuous smooth line is the least squares fit of a double Gaussian distribution to the histogram. The difference between the means of the two peaks is the single channel current. The single channel conductance was calculated according to eqn (4) (0·65 ± 0·04 pS, $n = 5$).

Homomeric ρ1 GABA receptor has a very low single channel chord conductance

Figure 4*A* shows an example of a GABA-activated single channel current in an outside-out patch pulled from an oocyte expressing ρ1 receptors. GABA (20 μM) elicited an inward single channel current in which channel activation persisted beyond the end of the GABA application. No channel openings were seen with switches to the control solution (data not shown), suggesting that single channel activities were induced by GABA and were not flow artifacts. Figure 4*B* shows the all-points amplitude histogram of the current trace in Fig. 4*A*. Two peaks in the histogram represent the open and closed states. The continuous smooth line is the best fit of a double Gaussian function to the data. The difference between the means of the two peaks is the single channel current from which the single channel chord conductance was calculated (0·65 ± 0·04 pS; $n = 5$).

In our recording conditions, the intracellular chloride concentration was 20 mM, which is much lower than that in mammalian cells and about one-half of the value we calculated in oocytes (43·5 mM). Therefore, it is likely that

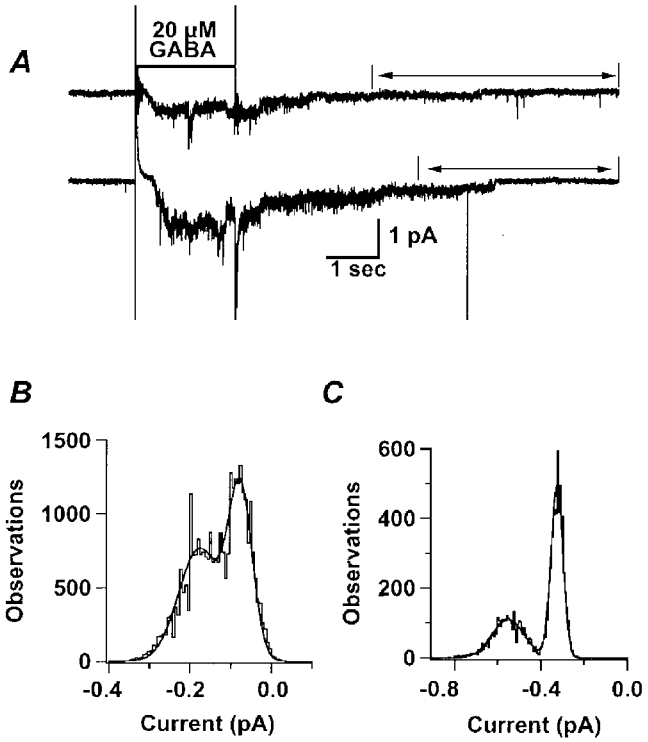

Figure 5. The single channel chord conductance is dependent upon $[Cl^-]_i$

A, examples of current traces in different solutions show that the current amplitude was higher when $[Cl^-]_i$ was increased. The upper trace shows a GABA-activated current in a multichannel patch held at −200 mV with a $[Cl^-]_i$ of 20 mM. The all-points amplitude histogram of this trace shows a single channel current of 0·10 pA under these conditions. In the lower trace, another multichannel patch shows a single channel chord conductance of 1·59 ± 0·24 pS ($n = 3$) when $[Cl^-]_i$ was increased to 100 mM. The all-points amplitude histograms, *B* and *C*, were derived from the portions of trace indicated by arrows in *A*.

the single channel chord conductance measured in our recording conditions would be lower than the conductance measured in physiological conditions, since single channel conductance of GABA receptors is dependent on chloride activity (Bormann *et al.* 1987). Figure 5 shows that when $[Cl^-]_i$ was 100 mM, the single channel current was larger than in 20 mM. The upper trace of Fig. 5*A* is from a multichannel patch induced by 20 μM GABA, recorded in 20 mM Cl^-_i with the membrane voltage clamped to −200 mV. The driving force in this case was −158 mV. After the end of GABA application, single current steps are apparent as the current decays to baseline. The lower trace in Fig. 5*A* is from a multichannel patch induced by the same concentration of GABA, but recorded in 100 mM Cl^-_i at a holding potential of −140 mV. Though the driving force in the lower trace was smaller (−138 mV), the current step was larger than that seen in the upper trace, suggesting a larger single channel chord conductance. Figure 5*B* is the all-points amplitude histogram for a segment (from 6 s to the end) of the upper trace in Fig. 5*A*. The difference between the two peaks of a double Gaussian fit was 0·10 pA, which represents the single channel current. Figure 5*C* is the all-points amplitude histogram for a segment (from 7 s to the end) of the lower trace. The single channel current in this case was 0·23 pA. Note the larger single channel current in the higher chloride solution. The calculated value of the single channel chord conductance from three patches with 100 mM Cl^-_i was 1·59 ± 0·24 pS.

Ensemble average of single channel currents has a time course similar to the macroscopic current

If the single channel currents we recorded represent the unitary conductance responsible for macroscopic GABA currents, then the ensemble average should have a time course similar to that of the macroscopic current. Figure 6*A* shows the single channel current traces from one outside-out patch activated repeatedly by 20 μM GABA. In most of the traces, GABA-induced channel openings had latencies that varied somewhat, and these channel openings lasted longer than the GABA applications. Occasionally, there was no current response to the GABA application. The bottom trace is the ensemble average of these single channel currents. A comparison of the upper and lower traces in Fig. 6*B* reveals the similarity of time courses of the ensemble and macropatch currents, respectively. This further supports the conclusion that the single channel events observed were ρ1 $GABA_C$ receptor openings.

GABA-induced openings can be blocked by picrotoxin

Figure 7 shows that the GABA-induced single channel currents were blocked by picrotoxin, which is expected for $GABA_C$ receptors (Cutting *et al.* 1991). The application of 20 μM GABA induced an inward current, which could be blocked when perfusion was briefly switched to GABA (20 μM) plus picrotoxin (100 μM). There were some brief openings during the picrotoxin application. The mean open time we observed from 43 GABA-induced channel openings in the absence of picrotoxin from 6 patches was 3·2 ± 0·8 s.

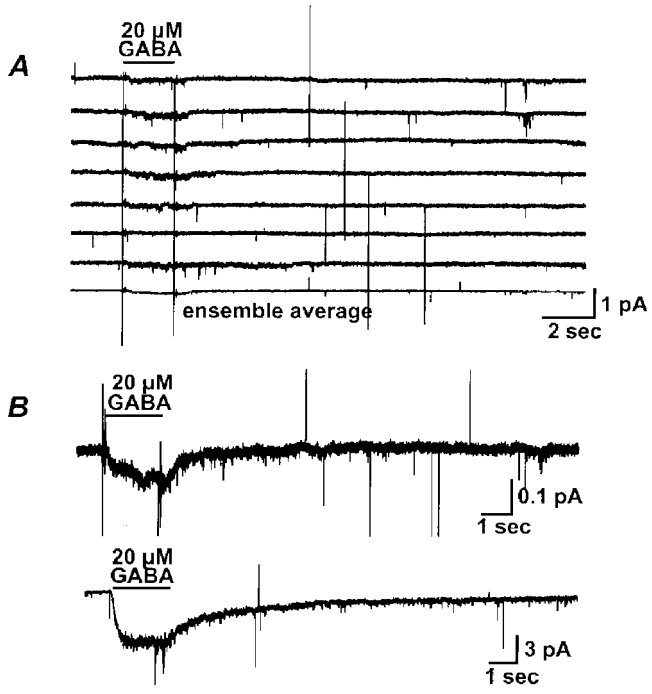

Figure 6. Ensemble average of single channel currents has a time course similar to the macroscopic current

A, representative current traces of 20 μM GABA-activated single channel activity from a single patch are shown; the bottom trace is the average of 12. The membrane voltage of the patch was clamped to −200 mV. GABA (20 μM) was applied through a computer-controlled piezo fast-switching system for 2 s. *B*, comparison of the ensemble average with the GABA response in a macropatch. The upper trace is the same ensemble average from *A*, on a different scale. The lower trace is the GABA-induced current in a macropatch from an oocyte expressing ρ1 GABA receptors.

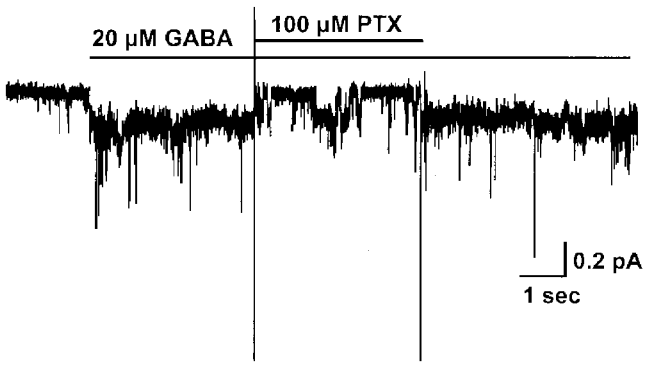

Figure 7. GABA-induced single channel current can be blocked by picrotoxin

Application of 20 μM GABA to an outside-out patch excised from an oocyte expressing ρ1 GABA receptors induced an inward current, which was blocked when perfusion was briefly switched to GABA (20 μM) plus picrotoxin (100 μM). The holding potential was −200 mV with a $[Cl^-]_i$ of 20 mM. Note that although the current returns to baseline during the picrotoxin application, some brief channel openings were evident. After removal of the antagonist, the GABA-induced current recovered.

Picrotoxin shortened the mean open time of the single channel events, which is one of the features of this channel blocker (Inomata *et al.* 1988; Inoue & Akaike, 1988). The mean open time in the presence of 100 μM picrotoxin was 0·07 ± 0·01 s (77 openings from 3 patches).

DISCUSSION

Permeability and pore size

Like the $GABA_A$ receptor, the homomeric ρ1 receptor displayed a marked selectivity for anions. Chloride is the primary physiologically relevant anion, but thiocyanate, iodide, nitrate, bromide, formate, bicarbonate and acetate all have measurable permeabilities. Comparison of the measurements in this study with those previously reported in spinal cord neurons (Bormann *et al.* 1987) shows that the ρ1 receptor is considerably more permeable to SCN^-, I^-, NO_3^-, Br^-, For^- and HCO_3^- than the $GABA_A$ receptor (Fig. 3). Relative permeabilities can be used in conjunction with the Stokes diameters of ions to predict the size of a pore. A plot of Stokes diameter (from the limiting ion conductance in water at 22 °C and the Einstein–Stokes relation, Robinson & Stokes, 1959) *versus* relative permeability is shown in Fig. 8. Fitting these plots with eqn (3) shows that the $\alpha1\beta2\gamma2$L receptor pore size is 0·56 nm, which is the same as the estimate of 0·56 nm for $GABA_A$ receptors from native spinal neurons (Bormann *et al.* 1987). The ρ1 homomeric receptor has a pore that is 0·61 nm in diameter, which is slightly larger than that of native (Bormann *et al.* 1987; Fatima-Shad & Barry, 1993) or recombinant (Fig. 8) $GABA_A$ receptors.

Ion selectivity and permeation

Ions are thought to enter the pore based on electrostatic attractions at the mouth. An initial selection process occurs at this point; molecules of the wrong charge are repelled from the pore opening, while those of the permeant charge are attracted. After an ion has entered the pore, additional selection may occur based on size exclusion and affinity to binding site(s) within the pore. These binding sites may occur along the length of the pore and would allow for more specific selection that may include factors like the size and shape of the molecule, as well as the charge (Dani, 1986). It is reasonable to conclude that the permeability differences we see between the ρ1 receptor and the $GABA_A$ receptor are due to differences in these interior binding sites. Although the amino acid sequence homology among the ρ1, α1, β2 and γ2 subunits is high in the putative second transmembrane domain, there are amino acid differences in this region as well. In fact, it may be possible to use domain swap and site-directed mutagenesis techniques to determine which residues control permeability.

It has been previously shown that ions with high permeabilities have a low conductance and vice versa (Bormann *et al.* 1987). In the case of an ion that gives high conductance measurements, time spent bound to the channel pore will be relatively brief, allowing many ions to cross the channel quickly. Low conductance/high permeability ions may remain bound for longer periods of time, slowing their travel through the pore, and perhaps blocking access to other ions that may be present. Thus, throughput of the channel is inversely related to the strength of each ion's association with the internal binding site(s) and to the number of binding sites in the pore. In the homomeric ρ1 receptor, the high permeabilities to thiocyanate, iodide, nitrate and bromide indicate that this receptor pore has a comparatively strong association with these ions.

The rank order of anion permeability of ρ1 receptors follows the Hofmeister series, which describes the behaviour of a series of ions in various physical/chemical interactions, including how the ions interact with water and with other molecules (Dani *et al.* 1983; Collins & Washabaugh, 1985). Although other possibilities exist, the fact that the observed order of permeability is the same as the Hofmeister series may be related to the increasing organization of the hydration sphere around each ion in solution, thus altering ionic interactions with the pore.

Expression system seems to have no effect on permeability

It has been previously shown that expression in different host cell types, particularly those that are not mammalian, can affect channel properties (Lewis *et al.* 1997). It is likely

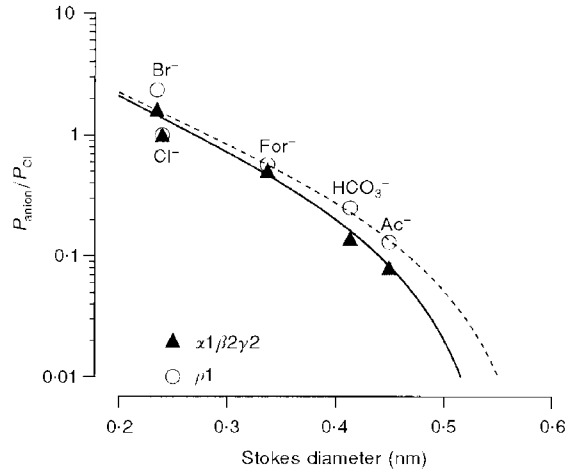

Figure 8. The ρ1 $GABA_C$ pore diameter is larger than that of the $\alpha1\beta2\gamma2$L $GABA_A$ receptor

The anionic permeabilities relative to chloride from Table 1 were plotted against the Stokes diameters of the ions (determined from the limiting conductances, Robinson & Stokes, 1959). A fit of eqn (3) using the permeabilities of the larger anions (chloride, formate, bicarbonate, and acetate) gave a pore size of 0·61 nm. This is larger than the estimated $\alpha1\beta2\gamma2$L $GABA_A$ receptor pore size of 0·56 nm.

that different cell types, especially those from different species, may process proteins differently in terms of glycosylation, phosphorylation or other factors that can affect channel function. We therefore included an examination of a typical $\alpha\beta\gamma$ $GABA_A$ receptor combination. Essentially no difference was seen in the relative permeability of this receptor isoform expressed in oocytes compared to the relative permeabilities measured in native spinal cord neurons (Fig. 3). It appears that expression in *Xenopus* oocytes does not significantly affect $GABA_C$ receptor permeability. In addition, the relative permeability of selected ions of ρ1 receptors in HEK293 cells was very similar to that seen in oocytes (Table 2), indicating that the results of this study are not unique to a particular expression system.

Single channel properties

Our measurement of the single channel chord conductance of homomeric ρ1 receptors was $0{\cdot}65 \pm 0{\cdot}04$ pS. We found that an extreme holding potential (−200 mV) was required to resolve the very small channel openings. Since the whole-cell current–voltage relationship was linear (Fig. 1), the measurement of single channel chord conductance was not affected by the holding potential. The very small single channel chord conductance and high open probability that we saw in ρ1 homomeric GABA receptors made it difficult to analyse single channel kinetics. Nevertheless, we estimated a mean open time of $3{\cdot}2 \pm 0{\cdot}8$ s. This suggests that ρ1 homomeric receptors have slow kinetics, in good agreement with the macroscopic current (Amin & Weiss, 1994).

In order to facilitate seals, potassium fluoride was used in the intracellular solution, reducing $[Cl^-]_i$ to 20 mM. It has been demonstrated that the single channel conductance of the $GABA_A$ receptor is dependent upon chloride activity with smaller single channel conductances in reduced-chloride solutions (Bormann *et al.* 1987). The single channel chord conductance measured at an intracellular chloride concentration of 100 mM was more than two-fold higher than that measured with $[Cl^-]_i$ of 20 mM (Fig. 5). This suggests that the ρ1 homomeric GABA receptor is similar to $GABA_A$ receptors in terms of the dependence of single channel conductance on chloride activity, which is probably due to multiple ion binding sites within the pore (Bormann *et al.* 1987).

Comparison to other studies

Although it is clear that permeability varies in the same order as the Hofmeister anions, the permeability values for homomeric ρ1 receptors we show here are somewhat greater than those previously reported by DelRaso *et al.* (1996). Notwithstanding, our relative permeabilities of $\alpha1\beta2\gamma2$L receptors in this *Xenopus* expression system are in very good agreement with the permeabilities reported for native receptors in spinal cord neurons (Bormann *et al.* 1987). Perhaps more importantly, our comparison of permeability and pore size of $\alpha1\beta2\gamma2$L and ρ1 receptors clearly shows that ρ1 receptor pores are larger than those of $\alpha1\beta2\gamma2$L receptors. Permeabilities have also been measured in dissociated retinal bipolar cells. In this preparation, the pore size of $GABA_C$ receptors was estimated at 0·51 nm (Feigenspan & Bormann, 1994). This value is smaller than the 0·61 nm we report here for ρ1 homomers. Based on pore sizes, it seems likely that the native retinal $GABA_C$ receptor previously reported (Feigenspan *et al.* 1993) may be composed of some other ρ subunit or perhaps a heteromeric arrangement of subunits.

Our estimate of the single channel chord conductance of human ρ1 receptors is in good agreement with the 1–5 pS (Pan *et al.* 1997) reported for the rat ρ1 receptor. This is not surprising since rat and human ρ1 subunits have amino acid sequences that are identical in all four transmembrane segments (Zhang *et al.* 1995). However, another report of the single channel conductance in human ρ1 receptors expressed in *Xenopus* oocytes is more than 30-fold higher than the value we observed (Lu, 1997). The reason for this discrepancy is not known, but it is clear that our results are in good agreement with those from rat ρ1 receptors.

It seems likely that receptors with $GABA_C$-like pharmacology studied in native tissue are not ρ1 homomers. The single channel conductance of 0·7 pS that we measure is smaller than the 7 pS that has been reported from rat retina bipolar cells (Feigenspan *et al.* 1993) or the 14 pS reported from rat hippocampal cells early in development (Martina *et al.* 1995). Additionally, the mean open time of 3·2 s we report here is considerably longer than the 150 ms from rat retinal bipolar cells (Feigenspan *et al.* 1993) or the 1·4 ms from hippocampus (Martina *et al.* 1995).

These data suggest that the ρ1 homomeric receptor is not likely to be the native retinal $GABA_C$ receptor previously described by Feigenspan (1993, 1994) or Martina *et al.* (1995) due to the differences in ionic permeabilities, pore size, single channel chord conductance and mean open time. The native $GABA_C$ receptor may be composed of some other ρ subunit or a heteromeric arrangement of subunits. Our data also show that permeabilities, pore sizes, single channel conductances, and mean open times differ between ρ1 receptors and $\alpha1\beta2\gamma2$L receptors. These differences will provide a basis for future investigation of the structural elements responsible for these properties.

Albrecht, B. E., Breitenbach, U., Stuhmer, T., Harvey, R. J. & Darlison, M. G. (1997). *In situ* hybridization and reverse transcription-polymerase chain reaction studies on the expression of the $GABA_C$ receptor ρ1- and ρ2-subunit genes in avian and rat brain. *European Journal of Neuroscience* **9**, 2414–2422.

Amin, J. & Weiss, D. S. (1994). Homomeric ρ1 GABA channels: activation properties and domains. *Receptors and Channels* **2**, 227–236.

Bormann, J., Hamill, O. P. & Sakmann, B. (1987). Mechanism of ion permeation through channels gated by glycine and γ-aminobutyric acid in mouse cultured spinal neurones. *Journal of Physiology* **385**, 243–286.

Collins, K. D. & Washabaugh, M. W. (1985). The Hofmeister effect and the behaviour of water at interfaces. *Quarterly Review of Biophysics* **18**, 323–422.

Cutting, G. R., Lu, L., O'Hara, B. F., Kasch, L. M., Montrose-Rafizadeh, C., Donovan, D. M., Schimada, S., Antonarakis, S. E., Guggino, W. B., Uhl, G. R. & Kazazian, H. H. (1991). Cloning of the γ-aminobutyric acid (GABA) ρ1 cDNA: A GABA receptor subunit highly expressed in the retina. *Proceedings of the National Academy of Sciences of the USA* **88**, 2673–2677.

Dani, J. A. (1986). Ion-channel entrances influence permeation. Net charge, size, shape, and binding considerations. *Biophysical Journal* **49**, 607–618.

Dani, J. A., Sanchez, J. A. & Hille, B. (1983). Lyotropic anions. *Journal of General Physiology* **81**, 255–281.

DelRaso, N. J., Huang, Y. & Lu, L. (1996). Effects of chlorotrifluoroethylene oligomer fatty acids on recombinant GABA receptors expressed in *Xenopus* oocytes. *Journal of Membrane Biology* **149**, 33–40.

Enz, R., Brandstatter, J. H., Harveit, E., Wassle, H. & Bormann, J. (1995). Expression of GABA receptor ρ1 and ρ2 subunits in the retina and brain of the rat. *European Journal of Neuroscience* **7**, 1495–1501.

Enz, R., Brandstatter, J. H., Wassle, H. & Bormann, J. (1996). Immunocytochemical localization of the $GABA_C$ receptor rho subunits in the mammalian retina. *Journal of Neuroscience* **16**, 4479–4490.

Fatima-Shad, K. & Barry, P. (1993). Anion permeation in GABA- and glycine-gated channels of mammalian cultured hippocampal neurons. *Proceedings of the Royal Society* B **253**, 69–75.

Feigenspan, A. & Bormann, J. (1994). Differential pharmacology of $GABA_A$ and $GABA_C$ receptors on rat retinal bipolar cells. *European Journal of Pharmacology* **288**, 97–104.

Feigenspan, A., Wassle, H. & Bormann, J. (1993). Pharmacology of GABA receptor Cl^- channels in rat retinal bipolar cells. *Nature* **361**, 159–162.

Goldman, D. E. (1943). Potential, impedance, and rectification in membranes. *Journal of General Physiology* **27**, 37–60.

Hodgkin, A. L. & Katz, B. (1949). The effect of sodium ions on the electrical activity of the giant axon of the squid. *Journal of Physiology* **108**, 37–77.

Inomata, N., Tokutomi, N., Oyama, Y. & Akaike, N. (1988). Intracellular picrotoxin blocks pentobarbital-gated Cl^- conductance. *Neuroscience Research* **6**, 72–75.

Inoue, M. & Akaike, N. (1988). Blockade of γ-aminobutyric acid-gated chloride current in frog sensory neurons by picrotoxin. *Neuroscience Research* **5**, 380–394.

Kusama, T., Spivak, C., Whiting, P., Dawson, V., Schaeffer, J. & Uhl, G. (1993). Pharmacology of GABA ρ1 and GABA α/β receptors expressed in *Xenopus* oocytes and COS cells. *British Journal of Pharmacology* **109**, 200–206.

Lewis, T. M., Harkness, P. C., Sivilotti, L. G., Colquhoun, D. & Millar, N. S. (1997). The ion channel properties of a rat recombinant neuronal nicotinic receptor are dependent on the host cell type. *Journal of Physiology* **505**, 299–306.

Lu, L. (1997). Effect of substituting amino acids in extracellular disulfide loop on GABA ρ1 subunit function. *Brain Research* **756**, 1–8.

Martina, M., Strata, F. & Cherubini, E. (1995). Whole cell and single channel properites of a new GABA receptor transiently expressed in the hippocampus. *Journal of Neurophysiology* **73**, 902–906.

Martina, M., Virginio, C. & Cherubini, E. (1997). Functionally distinct chloride-mediated GABA responses in rat cerebellar granule cells cultured in a low-potassium medium. *Journal of Neurophysiology* **77**, 507–510.

Methfessel, C., Witzemann, V., Mishina, M., Numa, S. & Sakmann, B. (1986). Patch clamp measurements on *Xenopus laevis* oocytes: currents through endogenous channels and implanted acetylcholine receptor and sodium channels. *Pflügers Archiv* **407**, 577–588.

Ogurusu, T. & Shingai, R. (1996). Cloning of a putative γ-aminobutyric acid (GABA) receptor subunit ρ3 cDNA. *Biochimica et Biophysica Acta* **1305**, 15–18.

Pan, Z.-H., Zhang, D., Zhang, X. & Lipton, S. A. (1997) Agonist-induced closure of constituitively open γ-aminobutyric acid channels with mutated M2 domains. *Proceedings of the National Academy of Sciences of the USA* **94**, 6469–6495.

Polezani, L., Woodward, R. M. & Miledi, R. (1991). Expression of mammalian γ-aminobutyric acid receptors with distinct pharmacology in *Xenopus* oocytes. *Neurobiology* **88**, 4318–4322.

Robinson, R. A. & Stokes, R. H. (1959). *Electrolyte Solutions.* Butterworths, London.

Shimada, S., Cutting, G. & Uhl, G. R. (1992). γ-Aminobutyric acid A or C receptor? γ-Aminobutyric acid ρ1 receptor RNA induce bicuculline-, barbiturate-, and benzodiazepine-insensitive γ-aminobutyric acid responses in *Xenopus* oocytes. *Molecular Pharmacology* **41**, 683–687.

Sivilotti, L. & Nistri, A. (1989). Pharmacology of a novel effect of γ-aminobutyric acid on the frog optic tectum *in vitro*. *European Journal of Pharmacology* **164**, 205–212.

Strata, F. & Cherubini, E. (1994). Transient expression of a novel type of GABA response in rat CA3 hippocampal neurones during development. *Journal of Physiology* **480**, 493–503.

Wang, T., Guggino, W. & Cutting, G. (1994). A novel γ-aminobutyric acid receptor subunit (ρ2) cloned from human retina forms bicuculline-insensitive homooligomeric receptors in *Xenopus* oocytes. *Journal of Neuroscience* **14**, 6524–6531.

Wegelius, K., Pasternack, M., Hiltunen, J. O., Rivera, C., Kaila, K., Saama, M. & Reeben, M. (1998). Distribution of GABA receptor ρ subunit transcripts in the rat brain. *European Journal of Neuroscience* **10**, 350–357.

Yeh, H. H., Griggorenko, E. V. & Veruki, M. L. (1996). Correlation between a bicuculline-resistant response to GABA and $GABA_A$ receptor ρ1 subunit expression in single rat retinal bipolar cells. *Visual Neuroscience* **13**, 283–292.

Zhang, D., Pan, Z.-H., Zhang, X., Brideau, A. D. & Lipton, S.A. (1995). Cloning of a γ-aminobutyric acid type C receptor subunit in rat retina with a methionine residue critical for picrotoxinin channel block. *Proceedings of the National Academy of Sciences of the USA* **92**, 11756–11760.

Acknowledgements

This work was supported by National Institutes of Health grants MH11793 to V.E.W. and NS35291 and NS36195 to D.S.W.

Corresponding author

D. S. Weiss: Department of Neurobiology, University of Alabama at Birmingham, 1719 Sixth Avenue South, CIRC 410, Birmingham, AL 35294, USA.

Email: dweiss@nrc.uab.edu

Virginia E. Wotring and Yongchang Chang contributed equally to this work.